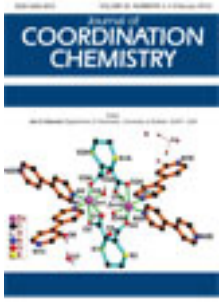

Journal of Coordination Chemistry
Publication details, including instructions for authors and subscription information:
http://www.tandfonline.com/loi/gcoo20

Review: Synthesis, characterization, and DNA-binding properties of Ru(II) molecular "light switch" complexes

C. Shobha Devi [a] & S. Satyanarayana [a]
[a] Department of Chemistry , Osmania University , Hyderabad 500 007 , India
Published online: 31 Jan 2012.

To cite this article: C. Shobha Devi & S. Satyanarayana (2012) Review: Synthesis, characterization, and DNA-binding properties of Ru(II) molecular "light switch" complexes, Journal of Coordination Chemistry, 65:3, 474-486, DOI: 10.1080/00958972.2011.649736

To link to this article: http://dx.doi.org/10.1080/00958972.2011.649736

Journal of Coordination Chemistry
Vol. 65, No. 3, 10 February 2012, 474–486

Review: Synthesis, characterization, and DNA-binding properties of Ru(II) molecular "light switch" complexes

C. SHOBHA DEVI and S. SATYANARAYANA*

Department of Chemistry, Osmania University, Hyderabad 500 007, India

(*Received 8 September 2011; in final form 21 November 2011*)

This article presents recent progress in our laboratory on the interactions of Ru(II) polypyridyl complexes with calf thymus DNA (CT-DNA). Mixed polypyridyl Ru(II) complexes $[Ru(L)_4(AIP)]^{2+}$ and $[Ru(L)_4PyIP]^{2+}$, where L is 4-amino pyridine and pyridine (AIP = 2-(9-anthryl)-1H-imidazo[4,5-f][1,10]phenanthroline; PyIP = 2-(1-pyrenyl)-1H-imidazo[4,5-f][1,10] phenanthroline), have been synthesized and characterized by elemental analysis, and physico-chemical methods such as ESI-MS, UV-Vis, IR, and NMR spectroscopic techniques. Electronic absorption titrations, fluorescence spectroscopy, viscosity measurements, and salt-dependent studies of CT-DNA in the presence of incremental amounts of all four Ru(II) complexes clearly demonstrate that all four complexes bind to DNA by intercalation. The DNA-binding affinities of these complexes follow the order $[Ru(4\text{-}APy)_4(PyIP)]^{2+} > [Ru(Py)_4PyIP]^{2+} > [Ru(4\text{-}APy)_4(AIP)]^{2+} > [Ru(Py)_4AIP]^{2+}$. Irradiation of pBR 322 DNA with these complexes results in nicking of the plasmid DNA. All four complexes were screened for antimicrobial activity. All complexes also exhibited DNA "light switch" properties. These results suggest that both ancillary ligand and intercalative ligand influence the binding of these complexes to DNA.

Keywords: Ru(II) complexes; Polypyridyl ligand; Fluorescence; Light switch effect; Photocleavage

1. Introduction

Recent trends in studies of metal complexes have focused on binding with DNA through intercalation [1–6]. DNA interstrand cross-linking agents comprise an extremely important class of clinical agents not only in the treatment of cancers, but also for diseases, such as psoriasis and various anemias. A quantitative understanding of factors that determine recognition of DNA sites would be valuable in the development of sensitive diagnostics and chemotherapeutics [7–10]. Several ruthenium complexes have developed as an alternative to Cisplatin (*cis*-diammine dichloro platinum(II), *cis*-$[PtCl_2(NH_3)_2]$) for potential use as therapeutic anticancer agents with lower toxicity than the platinum counterparts [11–14]. Structure–activity relationships of these complexes were studied in detail [15] giving new insight into understanding cytotoxicity of a series of Ru(II) anti-tumor complexes. The strong absorbance caused

*Corresponding author. Email: ssnsirasani@gmail.com

ISSN 0095-8972 print/ISSN 1029-0389 online
http://dx.doi.org/10.1080/00958972.2011.649736

by metal-to-ligand charge transfer (MLCT), luminescent characteristics, and their perturbations upon binding to DNA of the Ru(II) complexes provide practical means to explore their DNA-binding mechanisms. Ruthenium polypyridyl complexes are promising DNA probes due to their intense MLCT luminescence and excited state redox properties [16]. Certain other mixed-ligand ruthenium(II) complexes can be modified in 3-D to adopt to the DNA helix [17–19].

The majority of work on Ru(II) complexes emphasized on more intercalative ligands than ancillary ligands. However, a few works [20–23] have studied the role of ancillary ligands in polypyridyl Ru(II) complexes for their interaction with DNA. The ancillary ligand of polypyridyl ruthenium(II) complexes plays a key role in the spectral properties and interaction with DNA [24].

In most of the compounds described so far, the Ru(II) is bound to bidentate aromatic and polyaromatic ancillary ligands [25, 26]. Less attention has been paid to compounds containing monodentate ancillary ligands. In this contribution, we report synthesis and characterization of ruthenium polypyridyl complexes $[Ru(4\text{-}APy)_4(PyIP)]^{2+}$, $[Ru(Py)_4PyIP]^{2+}$, $[Ru(4\text{-}APy)_4(AIP)]^{2+}$, and $[Ru(Py)_4AIP]^{2+}$ which contain monodentate aromatic ancillary ligands. Their interactions with DNA were explored by electronic absorption, emission-quenching studies, viscosity, and salt-dependent studies. Effects of switching on and switching off light were also studied. This light switch effect is quite remarkable and provides the basis for a valuable photo-physical probe of nucleic acids. These complexes can intercalate into DNA base pairs and cleave the pBR 322 DNA with high activity upon irradiation. We have also tested all four complexes for their antimicrobial activity.

2. Experimental

2.1. *Materials*

All reagents and solvents were purchased commercially and used as received unless otherwise noted. $RuCl_3$, 1,10-phenanthroline monohydrate and pyridines were purchased from Merck. Calf thymus DNA (CT-DNA) was purchased from Aldrich and supercoiled pBR 322 DNA was obtained from Bangalore Genie. Doubly distilled water was used for preparing various buffers. Interactions of the complexes with DNA were studied in *tris*-buffer (5 mmol L^{-1} Tris-HCl, 50 mmol L^{-1} NaCl, pH 7.2). The DNA had a ratio of UV absorbance at 260 and 280 nm of about ~1.9 : 1, indicating that the DNA was sufficiently free of protein [27]. The concentration of DNA in nucleotide, i.e. phosphates or bases was determined spectrophotometrically using molar absorptivity of 6600 cm^{-1} (260 nm) [28, 29].

2.2. *Synthesis and characterization*

1,10-Phenanthroline-5,6-dione [30], AIP, PyIP [25], and $[Ru(L)_4Cl_2]$ were synthesized according to literature procedures [31]. Synthetic strategies of these ligands and their Ru(II) complexes are shown in figure 1.

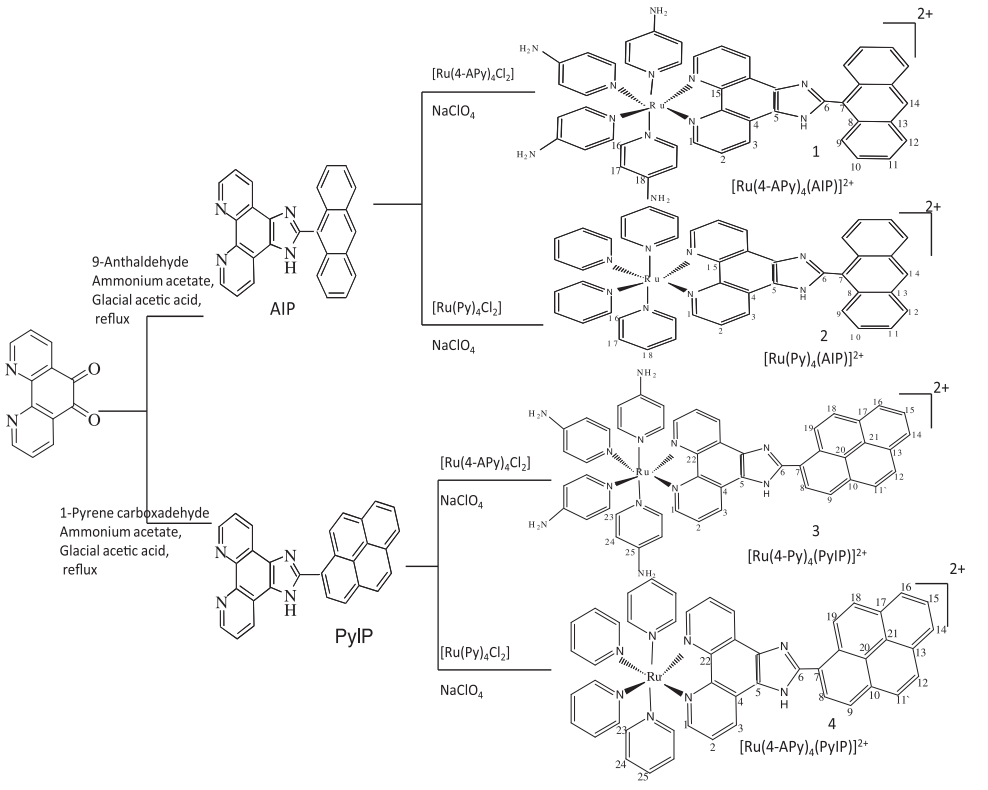

Figure 1. Synthetic routes for ligand and **1–4**.

2.2.1. Synthesis of $[Ru(4\text{-}APy)_4(AIP)](ClO_4)_2 \cdot 2H_2O$ (1). $[Ru(4\text{-}APy)_4(AIP)]$ was synthesized using a mixture of $[Ru(4\text{-}APy)_4Cl_2] \cdot 2H_2O$ (0.5 mmol L^{-1}) and AIP (0.5 mmol L^{-1}) refluxed in 25 mL ethanol and 15 mL water for 8 h under nitrogen to give a clear, red solution upon cooling; the solution was treated with a saturated aqueous solution of $NaClO_4$ to give a red precipitate. The red solid was collected and washed with small amount of water, ethanol, and ether, then dried in vacuum. Yield: 76%. Anal. Calcd for $C_{47}H_{43}N_{12}O_{10}Cl_2Ru$ (%): C, 50.94; H, 3.88; N, 15.17. Found (%): C, 50.89; H, 3.9; N, 15.2. ES^+-MS: calculated: 1107, found: 1108. IR (KBr) 3440 (broad) (N–H), 1655 (C=N), 1546 (C=C), 556 cm^{-1} (Ru–N). ^{1}H-NMR (DMSO-d_6, 400 MHz): δ 8.9 (d, 1H, H_{16}), δ 8.1 (m, 2H, H_1, H_3), δ 7.9 (d, 1H, H_{17}), δ 7.7 (m, 1H, H_9), δ 7.5 (m, 2H, H_2, H_{11}), δ 7.3 (t, 1H, H_{12}), δ 7.1 (d, 1H, H_{10}), δ 6.9 (s, 1H, H_{14}).

2.2.2. Synthesis of $[Ru(Py)_4(AIP)](ClO_4)_2 \cdot 2H_2O$ (2). This complex was obtained by a similar procedure to that described above; $[Ru(Py)_4Cl_2] \cdot 2H_2O$ (0.5 mmol L^{-1}) was used in place of $[Ru(4\text{-}APy)_4Cl_2] \cdot 2H_2O$. Yield: 65%. Anal. Calcd for $C_{47}H_{39}N_8O_{10}Cl_2Ru$ (%): C, 53.86; H, 3.72; N, 10.69. Found (%): C, 53.9; H, 3.8; N, 10.81. IR (KBr) 3450 (N–H), 1655 (C=N), 1561 (C=C), 550 cm^{-1} (Ru–N). ^{1}H-NMR (DMSO-d_6, 400 MHz): δ 9.0 (m, 2H, H_1, H_{16}), δ 8.9 (d, 1H, H_3), δ 8.2 (m, 2H, H_{17}, H_2), δ 7.9 (m, 3H, H_{18}, H_{10}, H_9), δ 7.8 (m, 2H, H_8, H_{11}), δ 7.7 (s, 1H, H_{14}). ^{13}C[^{1}H]-NMR (DMSO-d_6, 400 MHz):

δ 157 (1C, C_1), δ 155.7 (1C, C_{16}), δ 154.1 (1C, C_3), δ 150 (1C, C_{17}), δ 136.0 (2C, $C_{6,7}$), δ 135 (1C, C_{18}), δ 130.5 (2C, $C_{4,5}$), δ 129.0 (2C, $C_{8,13}$), δ 128.0 (1C, C_9), δ 125.0 (1C, C_2), δ 124.6 (1C, C_{10}), δ 124.0 (1C, C_{12}), δ 123.0 (1C, C_{14}), δ 120.4 (1C, C_{11}).

2.2.3. Synthesis of $[Ru(4\text{-}APy)_4(PyIP)](ClO_4)_2 \cdot 2H_2O$ (3). This complex was obtained by a similar procedure to that described above; PyIP (0.5 mmol L^{-1}) was used in place of AIP. Yield: 75%. Anal. Calcd for $C_{49}H_{44}N_{12}O_{10}Cl_2Ru$ (%): C, 51.94; H, 3.88; N, 14.84. Found (%): C, 52.01; H, 3.92; N, 14.91. IR (KBr) 3360 (broad) (N–H), 1643 (C=N), 1521 (C=C), 552 cm^{-1} (Ru–N) ^{1}H-NMR (DMSO-d_6, 400 MHz): δ 9.7 (d, 1H, H_1), δ 9.6 (d, 1H, H_{24}), δ 9.4 (m, 2H, H_2, H_{23}), δ 8.6 (d, 1H, H_3), δ 8.5 (m, 2H, $H_{8,9}$), δ 8.4 (m, 2H, $H_{11,19}$), δ 8.3 (m, 2H, $H_{12,18}$), δ 8 (d, 1H, H_{14}), δ 6.6 (s, 1H, H_{16}), δ 6.4 (m, 1H, H_{15}).

2.2.4. Synthesis of $[Ru(Py)_4(PyIP)](ClO_4)_2 \cdot 2H_2O$ (4). This complex was obtained by a similar procedure to that described above, $[Ru(Py)_4Cl_2] \cdot 2H_2O$ (0.5 mmol L^{-1}) was used in place of $[Ru(4\text{-}APy)_4Cl_2] \cdot 2H_2O$. Yield: 75%. Anal. Calcd for $C_{49}H_{41}N_8O_{10}Cl_2Ru$ (%): C, 54.85; H, 3.73; N, 10.44. Found (%): C, 54.93; H, 3.8; N, 10.54. ES^+-MS: calculated: 1072, found: 1070. IR (KBr) 3368 (broad) (N–H), 1650 (C=N), 1560 (C=C), 545 cm^{-1} (Ru–N) ^{1}H-NMR (DMSO-d_6, 400 MHz): δ 9.4 (s, 1H, H_1), δ 9.2 (m, 2H, H_2, H_3), δ 8.7 (s, 1H, H_{23}), δ 8.5 (m, 2H, H_{24}, H_{25}), δ 8.4 (m, 2H, $H_{8,11}$), δ 8.2 (m, 1H, H_{15}), δ 8.1 (m, 1H, H_{16}), δ 7.9 (m, 2H, H_9, H_{19}), δ 7.4 (s, 1H, H_{12}), δ 7.2 (s, 1H, H_{18}), 7.0 (s, 1H, H_{14}). $^{13}C[^1H]$-NMR (DMSO-d_6, 400 MHz): δ 157.7 (1C, C_1), δ 150.04 (1C, C_{24}), δ 136 (1C, C_3), δ 134.8 (1C, C_{25}), δ 132.15 (2C, $C_{4,5}$), δ 131.4 (2C, $C_{6,7}$), δ 131.02 (2C, $C_{21,22}$), δ 129.1 (1C, C_8), δ 128.9 (1C, C_9), δ 127.7 (1C, C_{11}), δ 127.05 (1C, C_{12}), δ 125.9 (1C, C_{18}), δ 125.2 (1C, C_{19}), δ 124.9 (1C, C_{20}), δ 124.2 (2C, $C_{14,15}$), δ 123.4 (1C, C_{16}) (figure 2).

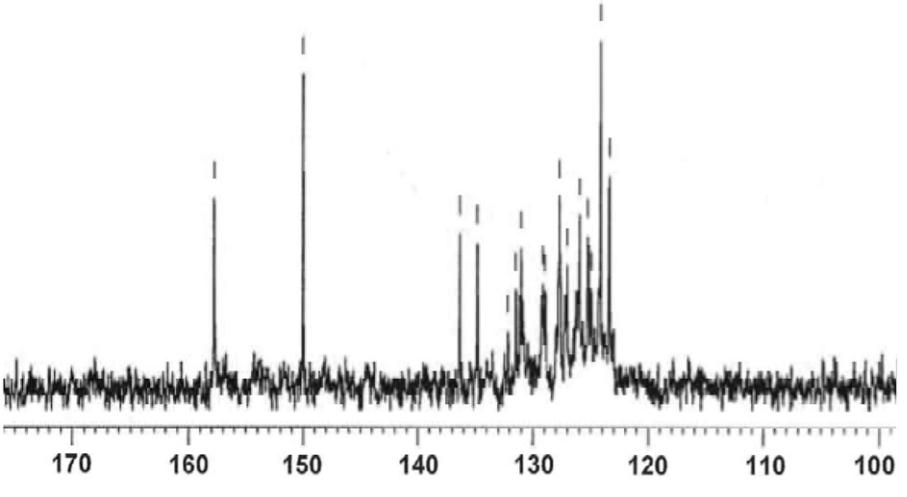

Figure 2. $^{13}C[^1H]$-NMR spectra of $[Ru(Py)_4(PyIP)]$.

2.3. *Physical measurements*

UV-Vis spectra were recorded with an Elico SL159 spectrophotometer. Infrared (IR) spectra were recorded as KBr discs on a Perkin-Elmer FT-IR-1605 spectrometer. ^{1}H and ^{13}C NMR spectra were recorded on a Bruker 400 MHz spectrometer with DMSO as solvent at RT and TMS as the internal standard. Electrospray ionization mass spectrometry (ESI-MS) mass spectra were recorded on an ESI-MS LCQ ion trap (Thermo Finningan, San Jose, CA, USA) mass spectrometer. Microanalyses (C, H, and N) were carried out with a Perkin-Elmer 240 elemental analyzer. Fluorescence measurements were performed on an Hitachi F-2500 spectrofluorimeter. Viscosity experiments were carried out on an Ostwald viscometer immersed in a thermostated water bath maintained at $30 \pm 0.1^{\circ}C$.

3. Results and discussion

3.1. *Absorbance titration experiment*

All four complexes were titrated with CT-DNA; the changes in spectral profiles during titration of $[Ru(4\text{-}APy)_4(PyIP)]^{2+}$ are shown in figure 3. As the DNA concentration

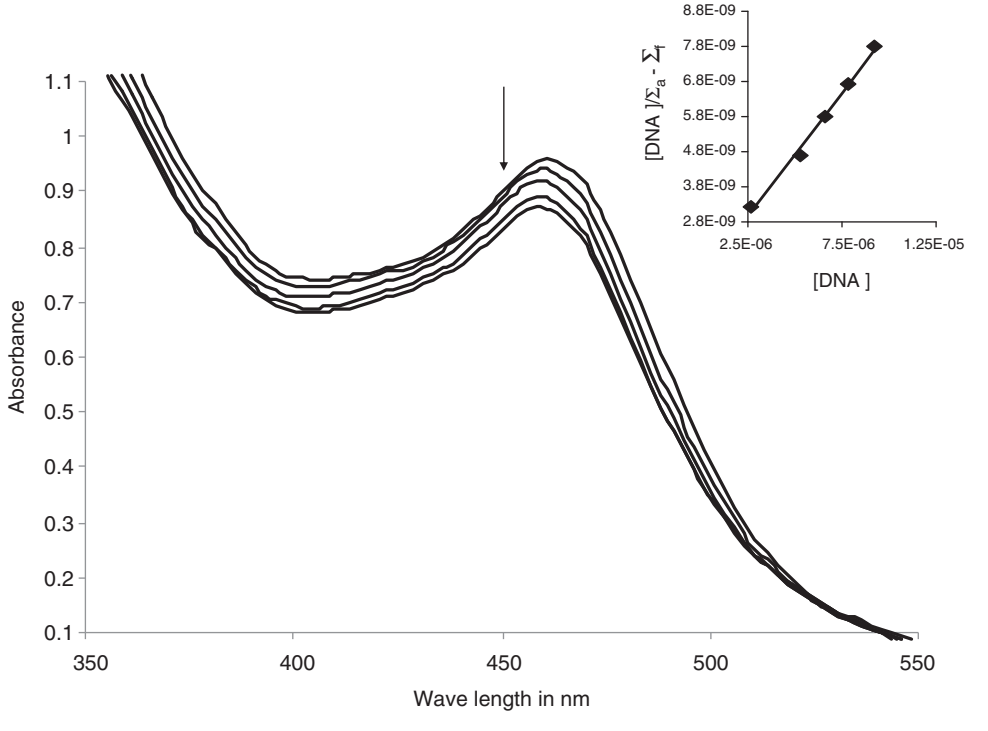

Figure 3. Absorption spectra of $[Ru(4\text{-}APy)_4(PyIP)]$ in *tris*-buffer upon addition of CT-DNA in the absence (top) and presence of CT-DNA (lower) the [complex] = 10–15 μmol L^{-1}. [DNA] = 0–120 μmol L^{-1}. Inset: plots of $[DNA]/(\varepsilon_a - \varepsilon_f)$ *vs.* [DNA] for the titration of Ru(II) complexes with DNA. The arrow shows change in absorption with increasing DNA concentration.

Table 1. DNA-binding (K_{sv}) data of Ru(II) complexes.

Complex	Absorption λ_{max} (nm)	Hypochromism	Absorption binding constant K_b $((mol\,L^{-1})^{-1})$	Emission binding constant	(K_{sv}) Only comp + DNA comp 1 : 50 1 : 200
$[Ru(4\text{-}APy)_4(PyIP)]$	471, 367, 325	11.50%	7.6×10^5	7.2×10^5	826 542 130
$[Ru(Py)_4PyIP]$	457, 382, 329	9.41%	6.41×10^5	6.3×10^5	752 379 101
$[Ru(4\text{-}APy)_4(AIP)]$	481, 385, 307	16.20%	3.36×10^5	3.5×10^5	483 245 75
$[Ru(Py)_4AIP]$	451, 398, 333	12.40%	2.5×10^5	2.6×10^5	432 211 45

increased (at constant concentration of complex), $[Ru(4\text{-}APy)_4(PyIP)]^{2+}$, $[Ru(Py)_4PyIP]^{2+}$, $[Ru(4\text{-}APy)_4(AIP)]^{2+}$, and $[Ru(Py)_4AIP]^{2+}$ show hypochromicity of 15.2, 12.5, 11.5, and 9.41%, respectively. Insignificant red shifts in the MLCT band at 471, 457, 481, and 451 of **1**–**4** were observed. To compare the DNA-binding affinities of all four complexes quantitatively, their intrinsic binding constants K_b to DNA were obtained by monitoring the changes of the MLCT absorbance at their respective wavelengths, according to the following equation [32]:

$$[DNA]/(\varepsilon_a - \varepsilon_f) = [DNA]/(\varepsilon_b - \varepsilon_f) + 1/K_b(\varepsilon_b - \varepsilon_f),$$

where [DNA] is the concentration of DNA in nucleotides, ε_a, ε_f, and ε_b are the extinction coefficient for the free Ru(II) complex, extinction coefficient of complex in the presence of DNA, and the extinction coefficient of the Ru(II) complex in the fully bound form, respectively. In plots of $[DNA]/[\varepsilon_a - \varepsilon_f]$ *versus* [DNA], K_b is given by the ratio of slope to intercept. Intrinsic binding constants K_b for all four complexes are given in table 1. The K_b values of all the complexes studied are in the order $[Ru(4\text{-}APy)_4(PyIP)]^{2+} > [Ru(Py)_4PyIP]^{2+} > [Ru(4\text{-}APy)_4(AIP)]^{2+} > [Ru(Py)_4AIP]^{2+}$. As PyIP possesses a greater planar area and extended π system, it penetrates more deeply into DNA base pairs, hence PyIP has a higher hypochromicity than that of AIP, and binding constants for **3** and **4** are higher than that of **1** and **2**. The difference in binding strengths of **1** and **2** or **3** and **4** is probably due to the difference in ancillary ligands. The NH_2 groups on pyridine in **1** and **3** may exert some additional interactions (may be H-bonding) with DNA base pairs and hence have higher binding constants. The K_b values of the complexes studied are smaller than that of Ru(II) complexes reported in the literature, such as $[Ru(Phen)_2(AIP)]$ ($K_b = 1.57 \times 10^6$ $(mol\,L^{-1})^{-1}$) and $[Ru(Phen)_2PyIP]$ ($K_b = 1.57 \times 10^6$ $(mol\,L^{-1})^{-1}$) [24]. This may also arise from larger planarity of the ancillary ligands, phenanthroline compared to pyridines.

3.2. *Luminescence spectroscopic studies*

The luminescence titration experiment was carried out in Tris buffer at ambient temperature [33]. Excitation peaks appeared at 475, 460, 485, and 456 nm and emission peaks at 541, 539, 584, and 593 nm for **1**, **2**, **3**, and **4**, respectively, as shown in figure 4. In all these complexes, emission intensity increases with the addition of CT-DNA. These spectral changes provide direct evidence for the interaction between the positively charged ruthenium complexes and the DNA polymer. Binding data were calculated from Scatchard plots of r/C_f *versus* r, where r is the binding ratio C_b/[DNA] and C_f is

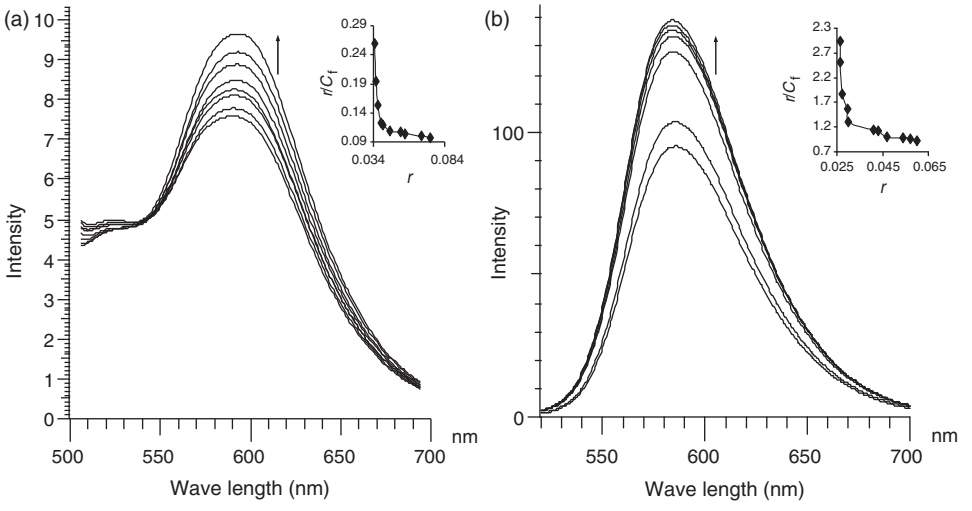

Figure 4. Emission spectra of $[Ru(4\text{-}APy)_4(PyIP)]$ (a), $[Ru(Py)_4PyIP]$ (b) in Tris-HCl buffer at 25°C upon addition of CT-DNA, $[Ru] = 20\,\mu mol\,L^{-1}$, $[DNA] = 0\text{–}120\,\mu mol\,L^{-1}$. The arrow shows the increase in intensity upon increasing CT-DNA concentrations.

the free ligand concentration. The binding constants calculated are consistent with the above absorption spectra results. The K values are given in table 1.

Hexacyanoferrate(II) is a suitable quencher to discriminate between differently bound ruthenium species with DNA. In the absence of DNA, the quenching of the fluorescence intensity of the Ru(II) complex by $[Fe(CN)_6]^{4-}$ is stronger, whereas in the presence of DNA quenching is weaker. The bound ruthenium complex is protected from the anionic quencher, since the highly negatively charged quencher is repelled by the negatively charged phosphate backbone of DNA. Figure 5 shows Stern–Volmer plots for luminescence quenching of **1**–**4** by hexacyanoferrate(II) in the absence and presence of DNA, respectively. The Stern–Volmer quenching constant K_{sv} can be determined by using the Stern–Volmer equation [34],

$$I_0/I = 1 + K_{sv}[Q],$$

where I_0 and I are the fluorescence intensities in the absence and presence of quencher, respectively, Q is the concentration of the quencher and K_{sv} is a linear Stern–Volmer quenching constant. In the quenching plot of I_0/I *versus* $[Q]$, K_{sv} is given by the slope. Figure 4 shows the Stern–Volmer plots for free complex in solution and the complex in the presence of increasing amounts of DNA. The K_{sv} values for all four complexes are given in table 1.

The stronger the binding of complex to DNA, the greater is the emission enhancement. Based on the emission enhancement data, the strength of complex binding with DNA is in the order **2** < **1** < **4** < **3**.

3.2.1. DNA light-switch behavior. Figure 6 gives the emission spectra of DNA-$[Ru(APy)_4(PyIP)]^{2+}$ in the absence and presence of Co^{2+}. From figure 6, after binding to DNA (switch on), the emission of DNA-$[Ru(APy)_4(PyIP)]$ can be quenched by

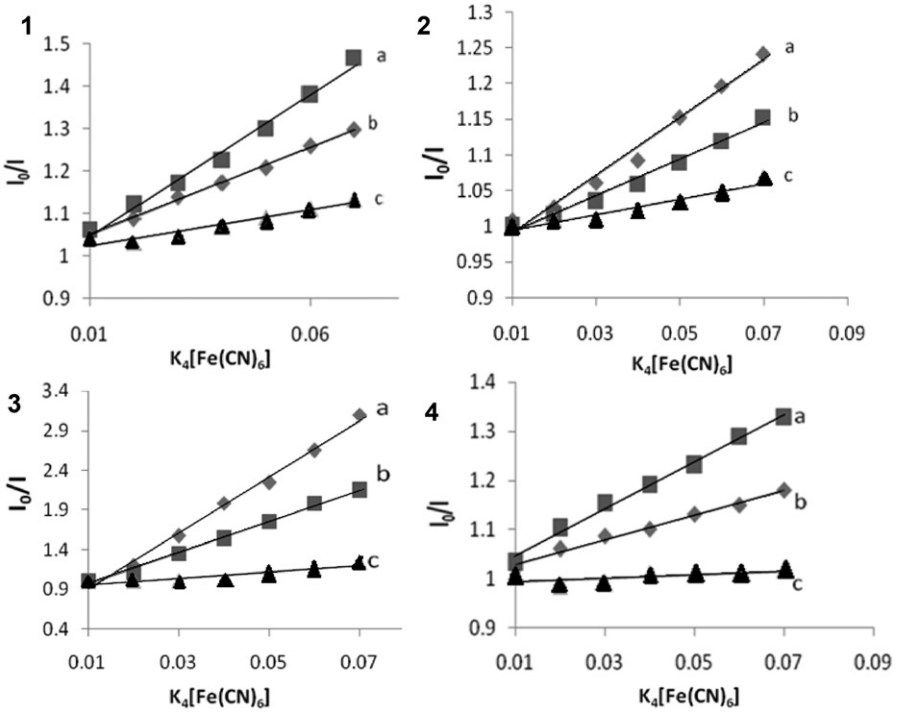

Figure 5. Emission quenching of [Ru(4-APy)$_4$(PyIP)] (**1**), [Ru(Py)$_4$PyIP] (**2**), [Ru(4-APy)$_4$(AIP)] (**3**), and [Ru(Py)$_4$AIP] (**4**) with $K_4[Fe(CN)_6]$ in the absence (a) and presence (b) [Ru] = 20 μmol L^{-1}, and excess of DNA (c).

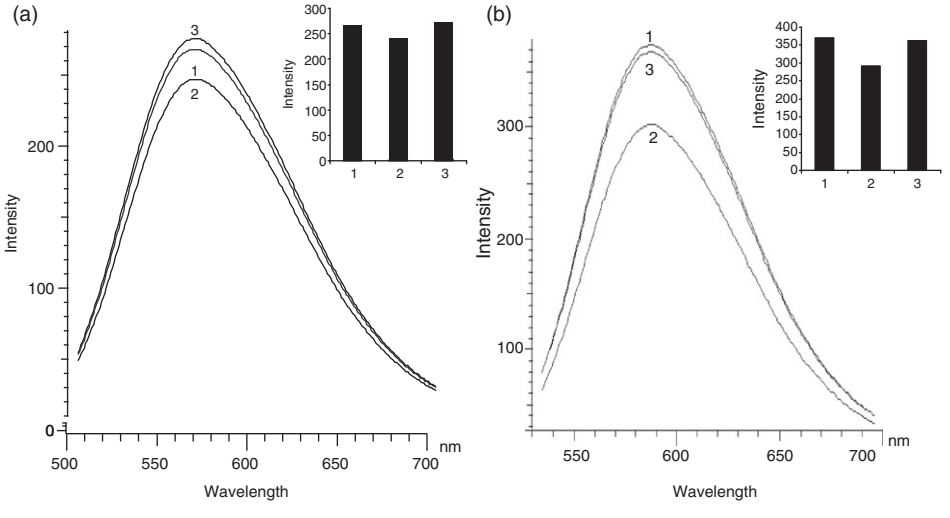

Figure 6. Luminescence changes of 0.01 mmol L^{-1} [Ru(PyIP)(APy)$_4$] in the presence of 0.2 mmol L^{-1} of DNA (a) and in the absence of 0.2 mmol L^{-1} DNA (b) (1), addition of 0.03 mmol L^{-1} Co^{2+} (2), and addition 0.03 mmol L^{-1} of EDTA (3).

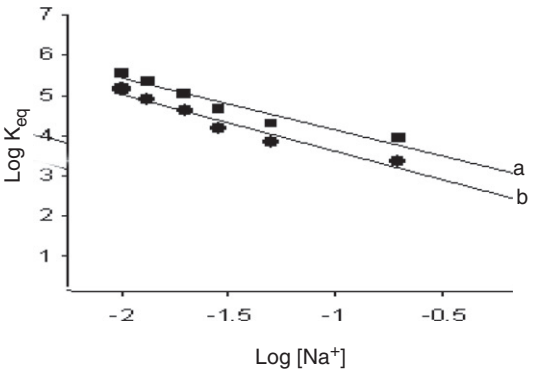

Figure 7. Salt dependence of the equilibrium binding constants for [Ru(4-APy)$_4$(PyIP)] (a) and [Ru(4-APy)$_4$(AIP)] (b). Slopes are −1.315 and −1.216, respectively.

cobalt(II), thus turning the light switch off [35, 36]. The addition of Co^{2+} (0.03 mmol L^{-1}) to the complex (0.01 mmol L^{-1}) bound to DNA (0.2 mmol L^{-1}) results in loss of luminescence due to the formation of a Co^{2+}–[Ru(APy)$_4$(PyIP)]$^{2+}$ heterometallic complex.

As shown in figure 6, on adding EDTA to the buffer system containing Co^{2+}–[Ru(APy)$_4$(PyIP)]$^{2+}$, the emission intensity of the complex is recovered again (light switch on). This indicates that the heterometallic complex Co^{2+}–[Ru(APy)$_4$(PyIP)] becomes free again due to EDTA–Co^{2+} complex formation. In this experiment adding 0.03 mmol L^{-1} of Co^{2+} decreased the intensity of [Ru(APy)$_4$(PyIP)], and on adding equimolar EDTA (0.03 mmol L^{-1}), the luminescence was recovered. Similar observations were obtained for all four complexes. The emission of the DNA-intercalated complex (light switch on) can be quenched by transition metal ions, thus turning the light switch off.

3.3. *Salt-dependent studies*

The polyelectrolyte theory quantitatively describes the thermodynamic linkage between cation and charged ligand binding to the DNA lattice. Cation and positively charged metal complex binding are thus thermodynamically linked and the binding of one influences the binding of the other. The dependency of the complex-DNA binding constant on cation concentrations is a manifestation of the thermodynamic linkage. As the concentration of salt (NaCl) increases, the binding constant decreases.

From the record theory, the slope of the lines in figure 7 provides an estimate of $Z\psi$, where ψ is the fraction of counter ions associated with each DNA phosphate ($\psi = 0.88$ for double-stranded B-form DNA) and Z is the charge on the complex. The data in figure 7 indicate that both Ru complexes carry a net charge of +2. Consequently, the slopes of the lines are greater than 1, −1.31, and −1.236 for **1** and **3**, respectively. These values are less than the theoretically expected value of $Z\psi = 2 \times 0.88 = 1.76$. Such lower values could arise from coupled anion release (from the ligand) or from changes in ligand or DNA hydration upon binding. By increasing the Na^+ concentration, the

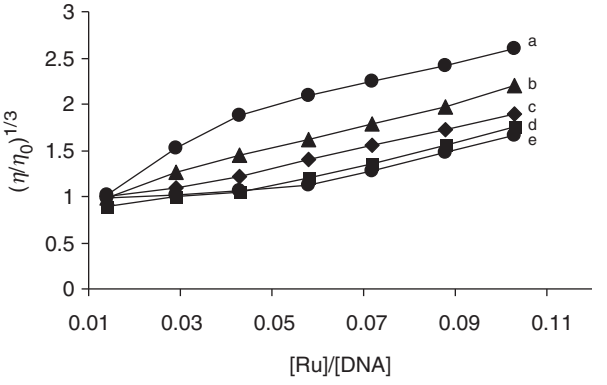

Figure 8. Effect of increasing amount of EB (a), $[Ru(4\text{-}APy)_4(PyIP)]$ (b), $[Ru(Py)_4PyIP]$ (c), $[Ru(4\text{-}APy)_4(AIP)]$ (d), and $[Ru(Py)_4AIP]$ (e) on relative viscosity of CT-DNA at $30 \pm 0.1°C$. The total concentration of DNA is $0.25\,mmol\,L^{-1}$.

relative binding affinities of the complexes decreased similar to that of proven intercalators [37] like ethidium bromide (EB).

3.4. *Viscosity measurements*

The measurement of viscosity of DNA is regarded as the least ambiguous and the most critical test of a DNA-binding model in solution in the absence of crystallographic structural data [3, 38]. A classical intercalation model demands that the DNA helix must lengthen as base pairs are separated to accommodate the binding ligand, leading to increase in viscosity of the DNA solution [3, 38]. The effects of $[Ru(4\text{-}APy)_4(PyIP)]^{2+}$, $[Ru(Py)_4PyIP]^{2+}$, $[Ru(4\text{-}APy)_4(AIP)]^{2+}$, $[Ru(Py)_4AIP]^{2+}$, and EB on the viscosity of rod-like DNA are shown in figure 8. As expected, EB increases the relative specific viscosity for the lengthening of the DNA double helix resulting from intercalation. The increased degree of viscosity may depend on the binding affinity to DNA (figure 8). These results also suggest that all complexes intercalate between the base pairs of DNA and parallel the results obtained by absorption, fluorescence, and quenching measurements.

3.5. *Antibacterial activity studies*

Recent reports have shown that ruthenium-based complexes have catalytic activity and also very good medicinal properties [39–42], so that synthesized ruthenium complexes were screened *in vitro* for their microbial activity against *Escherichia coli* and *Neurospora crassa* at $1.5\,mg\,mL^{-1}$ concentration by the standard disc method. The results were expressed as inhibition zone diameter (in mm) *versus* control (DMSO). The complexes were more effective against *E. Coli*. $[Ru(A\text{-}Py)_4(PyIP)]$ showed the highest activity (20 mm) (table 2). All these complexes showed less zone of inhibition with fungal species. The antimicrobial activity increased as the concentration of the compounds increased. Increase in the lipophilic character of the complex favors its

Table 2. Antibacterial activity of Ru(II) complexes.

	Bacterial species *E. coli*	Fungal species *N. crassa*
DMSO	Nil	Nil
$[Ru(4\text{-}APy)_4(PyIP)]$	20	17
$[Ru(Py)_4PyIP]$	15	12
$[Ru(4\text{-}APy)_4(AIP)]$	14	9
$[Ru(Py)_4AIP]$	4	1
Ampicillin	23–28	18–22

Zone of inhibition of diameter in (mm).

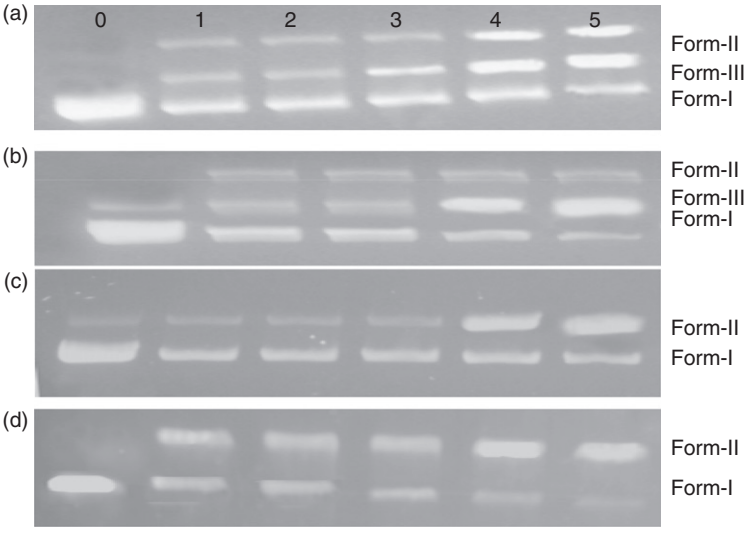

Figure 9. Photoactivated cleavage of pBR 322 DNA in the presence of $[Ru(4\text{-}APy)_4(PyIP)]$ (a), $[Ru(Py)_4PyIP]$ (b), $[Ru(4\text{-}APy)_4(AIP)]$ (c), and $[Ru(Py)_4AIP]$ (d) complexes after irradiation at 365 nm. Lane 0 control plasmid DNA (untreated pBR 322), lanes 1–5 addition of complexes 20, 40, 60, 80, and 100 μmol L^{-1}.

permeation through the lipid layer of the bacterial membrane, and therefore shows higher activity.

3.6. *Cleavage of plasmid DNA by Ru(II) complexes*

The ability of the present complexes to cleave DNA was studied by gel electrophoresis using pBR 322 DNA. When circular plasmid DNA is subject to electrophoresis, relatively fast migration will be observed for the intact supercoil form (Form-I). If scission occurs on one strand (nicking), the supercoil will relax to generate a slower moving open circular form (Form-II). If both strands are cleaved, a linear form (Form-III) that migrates between Form-I and Form-II will be generated [43]. In figure 9 the gel electrophoresis pattern of pBR 322 DNA is shown after incubation with **1**–**4** and

irradiation at 365 nm. No DNA cleavage was observed for the control in which a metal complex was absent (lane 0). With increasing concentration of the Ru(II) complexes (lanes 1–5), the amount of Form-I diminished gradually, whereas Form-II increased and Form-III was also produced. Under comparable experimental conditions, **3** exhibits more effective DNA cleavage activity than the other complexes. This may be related to the molecular structure of these complexes, which has been testified in another case [44].

4. Conclusions

Four Ru(II) complexes have been synthesized and characterized. Binding of these complexes to CT-DNA has been investigated by electronic absorption titration, steady state emission, viscosity, and salt-dependent studies. The results suggest that all the complexes bind to DNA in an intercalative mode. When irradiated at 365 nm, the four Ru(II) complexes were efficient photocleavers. Our studies led us to conclude that, as all four complexes are intercalators, they may be useful as a practical probe of DNA sequence or conformation. All the complexes show effects of light being switched on and switched off.

Acknowledgments

The Council of Scientific and Industrial Research (CSIR), New Delhi, India, is gratefully acknowledged for the financial support in the form of a Junior Research Fellow to C. Shobha Devi.

References

[1] E.C. Long, J.K. Barton. *Acc. Chem. Res.*, **23**, 271 (1990).
[2] D.S. Sigman, A. Mazumder, D.M. Perrin. *Chem. Rev.*, **93**, 2295 (1993).
[3] S. Satyanarayana, J.C. Dabrowiak, J.B. Chaires. *Biochemistry*, **32**, 2573 (1993).
[4] B.P. Hudson, C.M. Dupureur, J.K. Barton. *J. Am. Chem. Soc.*, **117**, 9379 (1995).
[5] (a) P. Lincoln, A. Broo, B. Norden. *J. Am. Chem. Soc.*, **118**, 2644 (1996); (b) E. Tuite, P. Lincoln, B. Norden. *J. Am. Chem. Soc.*, **119**, 239 (1997).
[6] C.M. Dupureur, J.K. Barton. *J. Am. Chem. Soc.*, **116**, 10286 (1994).
[7] D.T. Odom, C.S. Parker, J.K. Barton. *Biochemistry*, **38**, 5155 (1999).
[8] C. Metcalfe, J.A. Thomas. *Chem. Soc. Rev.*, **32**, 215 (2003).
[9] E.M. Boon, N.M. Jackson, M.D. Wightman, S.O. Kelley, M.G. Hill, J.K. Barton. *J. Phys. Chem. B*, **107**, 11805 (2003).
[10] V.C. Rucker, A.R. Dunn, S. Sharma, P.B. Dervan, H.B. Gray. *J. Phys. Chem. B*, **108**, 7490 (2004).
[11] M.J. Clarke. In *Metal Complexes in Cancer Chemotherapy*, B.K. Keppler (Ed.), p. 129, VCH, Weinheim (1993).
[12] B.K. Keppler, K.G. Lipponer, B. Stenzel, F. Kratz. In *Metal Complexes in Cancer Chemotherapy*, B.K. Keppler (Ed.), p. 187, VCH, Weinheim (1993).
[13] M.J. Clarke, F. Zhu, D.R. Frasca. *Chem. Rev.*, **99**, 2511 (1999).
[14] G. Sava, A. Bergamo. *Int. J. Oncol.*, **17**, 353 (2000).
[15] J.-C. Chen, L.-M. Chen, L.-C. Xu, K.-C. Zheng, L.-N. Ji. *J. Phys. Chem. B*, **112**, 9966 (2008).
[16] C.V. Kumar, J.K. Barton, N.J. Turro. *J. Am. Chem. Soc.*, **107**, 5518 (1985).

[17] A.M. Pyle, J.P. Rehmann, R. Meshoyrer, C.V. Kumar, N.J. Turro, J.K. Barton. *J. Am. Chem. Soc.*, **111**, 3051 (1989).
[18] D. Ossipov, P.I. Pradeepkumar, M. Holmer, J. Chattopadhyaya. *J. Am. Chem. Soc.*, **123**, 3551 (2001).
[19] P.K. Battacharya, J.K. Barton. *J. Am. Chem. Soc.*, **123**, 8649 (2001).
[20] Y. Xiong, L.-N. Ji. *Coord. Chem. Rev.*, **185**, 711 (1999).
[21] W.J. Mei, J. Liu, K.C. Zheng, L.J. Lin, H. Chao, A.X. Li, F.C. Yun, L.N. Ji. *Dalton Trans.*, 1352 (2003).
[22] J.-G. Liu, Q.-L. Zhang, X.-F. Shi, L.-N. Ji. *Inorg. Chem.*, **40**, 5045 (2001).
[23] L.-M. Chen, J. Liu, J.-C. Chen, C.-P. Tan, S. Shi, K.-C. Zheng, L.-N. Ji. *J. Inorg. Biochem.*, **102**, 330 (2008).
[24] M. Mariappan, B.G. Maiya. *Eur. J. Inorg. Chem.*, 2164 (2005).
[25] P. Nagababu, M. Shilpa, S. Satyanarayana, J.N.L. Latha, K.S. Karthikeyan, M. Rajesh. *Transition Met. Chem.*, **33**, 1027 (2008).
[26] P. Nagababu, D. Aravind Kumar, K. Laxma Reddy, K. Ashwini Kumar, Md.B. Mustafa, M. Shilpa, S. Satyanarayana. *Met.-Based Drugs*, Article ID 275084 (2008).
[27] J. Marmur. *J. Mol. Biol.*, **3**, 208 (1961).
[28] P.U. Maheswari, V. Rajendiran, M. Palaniandavar, R. Parthasarathi, V. Subramanian. *J. Inorg. Biochem.*, **100**, 3 (2006).
[29] M.E. Reichmann, S.A. Rice, C.A. Thomas, P. Doty. *J. Am. Chem. Soc.*, **76**, 3047 (1954).
[30] M. Yamada, Y. Tanaka, Y. Yoshimoto, S. Kuroda, I. Shimo. *Bull. Chem. Soc. Japan*, **65**, 1006 (1992).
[31] B.P. Sullivan, D.J. Salmon, T.J. Mayer. *Inorg. Chem.*, **17**, 3334 (1978).
[32] A. Wolfe, G.H. Shimer, T. Mechan. *Biochemistry*, **26**, 6392 (1984).
[33] J.B. Chaires, N. Dattagupta, D.M. Crothers. *Biochemistry*, **24**, 3927 (1982).
[34] J.R. Lakowicz, G. Webber. *Biochemistry*, **12**, 4161 (1973).
[35] X.-W. Liu, Y.-M. Shen, J.-L. Lu, Y.-D. Chen, L. Li, D.-S. Zhang. *Spectrochim. Acta, Part A*, **77**, 522 (2010).
[36] M. Chen, H. Li, Q. Li, Z. Xu. *Spectrochim. Acta, Part A*, **75**, 1566 (2010).
[37] S. Satyanarayana, J.C. Dabrowiak, J.B. Chaires. *Biochemistry*, **31**, 9319 (1992).
[38] S. Satyanarayana, D. Suh, I. Fokt, T. Przewloka, W. Priebe, J.B. Chaires. *Biochemistry*, **35**, 7 (1996).
[39] K. Mikami, T. Korenaga, M. Terada, T. Ohkuma, T. Pham, R. Noyori. *Angew. Chem. Int. Ed. Engl.*, **38**, 495 (1999).
[40] M. Yamakawa, H. Ito, R. Noyori. *J. Am. Chem. Soc.*, **122**, 1466 (2000).
[41] C. Kaes, A. Katz, M.W. Hosseini. *Chem. Rev.*, **100**, 3553 (2000).
[42] C.S. Allardyce, P.J. Dyson, D.J. Ellis, S.L. Health. *Chem. Commun.*, 1396 (2001).
[43] J.K. Barton, A.L. Raphael. *J. Am. Chem. Soc.*, **106**, 2466 (1984).
[44] H. Chao, W.J. Mei, Q.W. Huang, L.N. Ji. *J. Inorg. Biochem.*, **92**, 165 (2002).